Tree Physiology 31, 1194–1203
doi:10.1093/treephys/tpr099

Research paper

Localized stem chilling alters carbon processes in the adjacent stem and in source leaves

Veerle De Schepper[1,3], Lynn Vanhaecke[2] and Kathy Steppe[1]

[1]Laboratory of Plant Ecology, Department of Applied Ecology and Environmental Biology, Faculty of Bioscience Engineering, Ghent University, Coupure Links 653, B-9000 Ghent, Belgium; [2]Laboratory of Chemical Analysis, Department of Veterinary Public Health and Food Safety, Faculty of Veterinary Medicine, Ghent University, Salisburylaan 133, B-9820 Merelbeke, Belgium; [3]Corresponding author (Veerle.DeSchepper@UGent.be).

Received April 5, 2011; accepted August 26, 2011; published online October 13, 2011; handling Editor Peter Millard

Transport phloem is no longer associated with impermeable pipes, but is instead considered as a leaky system in which loss and retrieval mechanisms occur. Local stem chilling is often used to study these phenomena. In this study, 5-cm-lengths of stems of 3-year-old oak trees (*Quercus robur* L.) were locally chilled for 1 week to investigate whether observations at stem and leaf level can be explained by the leakage-retrieval mechanism. The chilling experiment was repeated three times across the growing season. Measurements were made of leaf photosynthesis, carbohydrate concentrations in leaves and bark, stem growth and maximum daily stem shrinkage. Across the growing season, a feedback inhibition in leaf photosynthesis was observed, causing increased dark respiration and starch concentration. This inhibition was attributed to the total phloem resistance which locally increased due to the cold temperatures. It is hypothesized that this higher phloem resistance increased the phloem pressure above the cold block up to the source leaves, inducing feedback inhibition. In addition, an increase in radial stem growth and carbohydrate concentration was observed above the cold block, while the opposite occurred below the block. These observations indicate that net lateral leakage of carbohydrates from the phloem was enhanced above the cold block and that translocation towards regions below the block decreased. This behaviour is probably also attributable to the higher phloem resistance. The chilling effects on radial stem growth and carbohydrate concentration were significant in the middle of the growing season, while they were not at the beginning and near the end of the growing season. Furthermore, maximum daily shrinkages were larger above the cold block during all chilling experiments, indicating an increased resistance in the xylem vessels, also generated by low temperatures. In conclusion, localized stem chilling altered multiple carbon processes in the source leaves and the main stem by changing hydraulic resistances.

Keywords: carbohydrates, cold girdling, feedback inhibition of photosynthesis, phloem, *Quercus robur* L., seasonal variation, stem growth, sugar transport, translocation.

Introduction

Among plant biologists there is a consensus that phloem solutes are transported by mass flow, driven by a pressure difference between sources and sinks (cf. the Münch hypothesis; Münch 1930). In the course of time this hypothesis has been further refined and extended (van Bel 2003*a*): (i) both symplastic and apoplastic routes exist for the loading processes in the source phloem and the unloading processes in the sink phloem (e.g., Gamalei 2002, Lalonde et al. 2003, van Bel 2003*b*); and (ii) the transport phloem is leaky since solutes and solvent are continuously released and retrieved along the pathway (e.g., Minchin and Thorpe 1987, Ayre et al. 2003, van Bel 2003*c*). It is believed that this leakage-retrieval mechanism helps maintain a constant flow from sources to sinks

during times of changing supply and demand by using the local apoplast as a short-term sucrose buffer (Thorpe et al. 2005). The symplast (parenchyma and ray cells) is considered as the long-term carbohydrate pool which will be depleted or replenished whenever the short-term buffer is well depleted or replenished. The lateral carbohydrate transport to this long-term pool is controlled by the apoplast sucrose concentration, which is held relatively constant. Hence, the apoplast acts as an intermediate phase between the phloem tissue and the long-term symplastic pool (Thorpe et al. 2005).

Local chilling of the stem tissue is often used to study this leakage-retrieval mechanism in the transport phloem (Gould et al. 2004, McQueen et al. 2005). In most cases a short-term chilling event of several minutes to hours is applied to alter phloem conditions. These chilling experiments (Gould et al. 2004, Peuke et al. 2006) have illustrated that phloem flow stops immediately when chilling is applied, but that it then quickly recovers after some minutes even when chilling is maintained. This short-term blockage of the phloem pathway is probably induced by calcium-dependent sealing proteins which temporarily occlude the sieve elements when cooling occurs (Thorpe et al. 2010). The leakage-retrieval mechanism is, however, generally detected in long-term chilling experiments of several days: the carbohydrate concentration increases above the chilled zone, while it decreases in the stem zone below (Hannah et al. 2001, Peuke et al. 2006, Johnsen et al. 2007). In addition, a reduction in carbon allocation towards the roots is observed during chilling (Hannah et al. 2001, Johnsen et al. 2007). Some researchers (Lang and Minchin 1986, Peuke et al. 2006) suggested that cold temperatures inhibit the retrieval of carbohydrates into the phloem. According to Peuke et al. (2006), this hypothesis could be responsible for the leaked carbohydrates which accumulate partly in the symplastic pool of the stem tissue above the chilled zone. However, Hannah et al. (2001) argued that the absence of starch accumulation in the bark of the cooled region (Hannah et al. 2001, Peuke et al. 2006) does not support the inhibited retrieval hypothesis. Nevertheless, chilling experiments indicate that phloem translocation is influenced by cooling and support that the phloem pathway is influenced by lateral sugar leakage. Only a few studies (Johnsen et al. 2007) have so far investigated the integrated effects of local stem chilling at source and sink level. Because local chilling partially inhibits carbon translocation towards the roots and has similar although smaller effects as physical girdling, it is often called cold girdling (Hannah et al. 2001, Peuke et al. 2006).

The research questions of this study were: (i) what changes happen in the sources and sinks of woody trees when local stem chilling is applied; (ii) does the leakage-retrieval hypothesis allow one to explain any observed chilling effects; and (iii) will these chilling-induced changes vary across the growing season as suggested by Johnsen et al. (2007), who observed significant chilling effects at the end of the growing season only, when translocation towards the roots was highest? To answer these questions, we locally chilled young oak trees for 1 week at three different times across the growing season and studied the effects on carbon processes in the stem and in the source leaves.

Materials and methods

Plant materials and experimental set-up

Twenty-two 3-year-old oak trees (*Quercus robur* L.) were planted in 50-l containers in February 2010. The containers were filled with a potting mixture (LP502D, Peltracom NV, Ghent, Belgium) and fertilized with a slow-releasing NPK plus magnesium mix (Basacote Plus 6M, COMPO, Deinze, Benelux). The trees were placed in the greenhouse facilities of the Faculty of Bioscience Engineering of Ghent University, Belgium. At the beginning of the growing season the trees had a height of ~1.65 m and a stem diameter of about 1.2 cm. Half of the trees were subjected to local stem chilling, while the other half served as control trees. This local stem chilling was achieved by placing a cold-block collar around the stem at 30 ± 5 cm above the soil surface. Collars were made of plastic tubing coiled around the circumference seven times to enclose ~5 cm of the stem surface. Chilling was applied by circulating anti-freeze liquid through the collars supplied by a cooling system controlled at 0 °C. All plastic tubes were insulated with polyethylene foam to minimize heat exchange with the environment. The local chilling zone divided the stem in to an upper (*U*) and a lower stem zone (*L*) above and below the chilled zone.

The chilling experiment was repeated three times across the growing season (Table 1). These repetitions will henceforth be referred to as R1, R2 and R3. Each repetition consisted of a control period before chilling, a period in which local stem chilling was applied, and a recovery period after chilling. Since every period took ~1 week, the total measurement period of each repetition covered about 3 weeks. Non-destructive physiological variables were measured using the same trees during all three repetitions (five control trees and five chilled trees), while destructive samples for carbohydrate concentrations were taken on trees which were harvested after each repetition (two control trees and two chilled trees per repetition).

Table 1. Overview of the cold-girdling experiment across the growing season (day of the year (DOY)).

Repetition	Month	Measurement period (DOY)	Chilling period (DOY)
R1	May	122:143	129:136
R2	June	151:171	157:165
R3	September	234:257	241:252

Microclimate

A quantum sensor (Li-190S, Li-COR, Lincoln, NE, USA) was used to measure photosynthetic active radiation (PAR) above the canopy. Air temperature (T_{air}) was measured with a copper–constantan thermocouple (Omega, Amstelveen, the Netherlands), and relative humidity (RH) with a capacitive RH sensor (Hygroclip S, Rotronic, AG Schweiz, Bassersdorf, Switzerland). These two sensors were installed together above the canopy and used to calculate vapour pressure deficit of the air (VPD). Furthermore, stem temperature (T_{stem}) was measured at the position where chilling was applied using a copper–constantan thermocouple (Omega) installed at the bark surface beneath the cooling tubes.

Physiological leaf characteristics

Leaf gas exchange measurements were carried out between 10:00 and 14:00 with an infrared gas analyser system (LI-6400, Li-COR) to determine dark leaf respiration (R_d) and net leaf photosynthesis at 1000 PAR ($P_{n,1000}$), exposing the leaves at 0 and 1000 μmol PAR m^{-2} s^{-1} for about 10 minutes, respectively. Relative humidity in the leaf chamber was uncontrolled and equal to the humidity in the greenhouse, while the air temperature in the leaf chamber was controlled at 25 °C. External air was scrubbed of CO_2 and mixed with pure CO_2 to create a standard concentration of 400 μmol mol^{-1}. The air flow rate was set at 200 μmol s^{-1}.

Stem diameter variations

Stem diameter variations (ΔD) were measured using linear variable displacement transducers (LVDTs) (model 2.5 DF, Solartron Metrology, Leicester, UK). The LVDTs were attached to the stem by custom-made stainless-steel holders which do not require a temperature correction (Steppe and Lemeur 2004). One LVDT was attached per control tree, while two LVDTs were attached per chilled tree: the first LVDT ~2 cm above the chilled zone and the second LVDT ~2 cm below the chilled zone. The average growth rate and the maximum daily shrinkage (MDS) were derived from these continuous measurements. Figure 1 shows a typical example of how the average growth rate and MDS were calculated. Average growth rate and average MDS were calculated for the periods before, during and after chilling for each repetition. The average growth rate of each period is derived from linear regressions made in Sigmaplot (Systat Software Inc., San Jose, CA, USA) (Figure 1). The linear regression was fitted to the maximum stem diameter values at night only, to eliminate the influence of daily stem shrinkage on stem growth rate. To deal with plant variability, the growth rate of each tree was normalized by dividing the growth rate of each period by the growth rate observed before chilling. The normalized growth rate was then averaged for the five control and the five chilled trees. In contrast, the average MDS of a period is the average of the daily MDSs during that period for the five control and five chilled trees.

Carbohydrate measurements

Bark and leaf samples for sugar and starch analysis were collected at the end of each period (before, during and after chilling) during the three repetitions. The bark of two control and two chilled trees was sampled. In the chilled trees, the bark was sampled in a region of 10 cm above and below the cooled zone. Simultaneously one leaf per tree was collected from five control and five chilled trees. The leaves sampled at the same time were analysed as one pooled sample for the control and chilled trees to increase sample weight. All samples were immediately frozen in liquid nitrogen and stored at −80 °C. Soluble sugars were extracted from the ground bark samples with 80% ethanol at 45 °C for 3 h, followed by centrifugation at 5000 *g* for 5 min. Glucose, fructose, sucrose and sorbitol were quantified using an Agilent 1100 high-performance liquid chromatography system (Agilent Technologies, Santa Clara, CA, USA) coupled to an Alltech 3300 electrochemical light scattering detector (Geneva, IL, USA) using acetonitrile:water (75:25) as eluent (Pollet et al. 2011). The remaining ethanol-insoluble

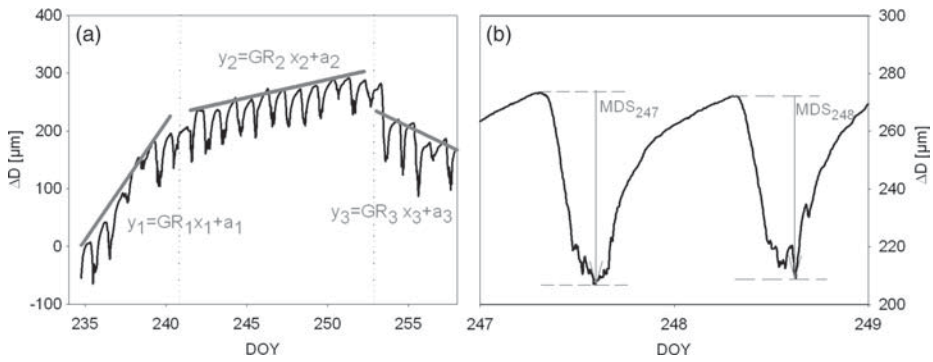

Figure 1. A typical example of a time series of stem diameter variations (ΔD) for a chilled tree, illustrating the definition of average growth rate (GR) and maximum daily shrinkage (MDS). Growth rate is calculated per period (1: before chilling; 2: during chilling, 3: after chilling) and is defined as the slope of the fitted linear curve (a). MDS is illustrated by the arrow (b).

material was washed twice with 80% ethanol and the residual pellet was treated with 1 M HCl for 2 h at 95 °C to achieve starch hydrolysis. Starch concentration, expressed as glucose equivalents, was determined spectrophotometrically (Genesys 10UV, Spectronic Analytical Instruments, Leeds, UK) at 340 nm by the enzymatic reduction of $NADP^+$. The total soluble sugar concentration was calculated as the sum of fructose, glucose, sucrose and sorbitol. To deal with plant variability and allow interplant comparison, concentrations were normalized by dividing the actual concentration by the concentration found before chilling.

Results

Microclimate

The microclimate in the greenhouse varied between and during the three repetitions (Figure 2). Photosynthetic active radiation, T_{air} and VPD (Figure 2a–c) increased gradually during R1. During R3, T_{air} and VPD gradually increased, while PAR did not follow this trend. This highly dynamic microclimate emphasizes that a comparison with control trees is necessary to identify the chilling effects during the different measurement periods. The impact of local stem chilling is clearly visible in the dynamics of T_{stem} (Figure 2d). During the chilling period, T_{stem} of the chilled trees was ~3 °C, which was ~20 °C lower than T_{stem} of the control trees.

Leaf photosynthesis and dark respiration

The stem chilling effects became clear when leaf R_d and $P_{n,1000}$ ratios of chilled to control trees were considered (Figure 3a and b). According to these ratios, the R_d of chilled trees significantly increased compared with control trees (Figure 3a), while $P_{n,1000}$ showed a decreasing but non-significant trend (Figure 3b).

Stem diameter variations

The stem growth rate of control trees gradually increased during R1 (Figure 4a), illustrating the beginning of the growing season. During R3 the growth rate gradually decreased (Figure 4c). The effects of local stem chilling became clear by looking at the normalized stem growth (Figure 4d–f). Chilling events had no significant effects on the normalized stem growth during R1 (Figure 4d). However, chilling had a significant effect on normalized growth rate in both the lower and the upper stem zone during R2 and R3 (Figure 4e and f). During chilling in R2 (Figure 4e), the normalized growth rate was significantly higher for *U* compared with *L*. After chilling, growth increased significantly in *U* and to a lesser extent in *L*. Chilling in R3 caused the growth of *U* and *L* to reduce significantly compared with the control tree (Figure 4f). After this chilling period, the lower growth rate remained in *U* while it became negative in *L*.

In addition, local stem chilling had a significant effect on MDS (Figure 5). Maximum daily shrinkage in *U* during chilling

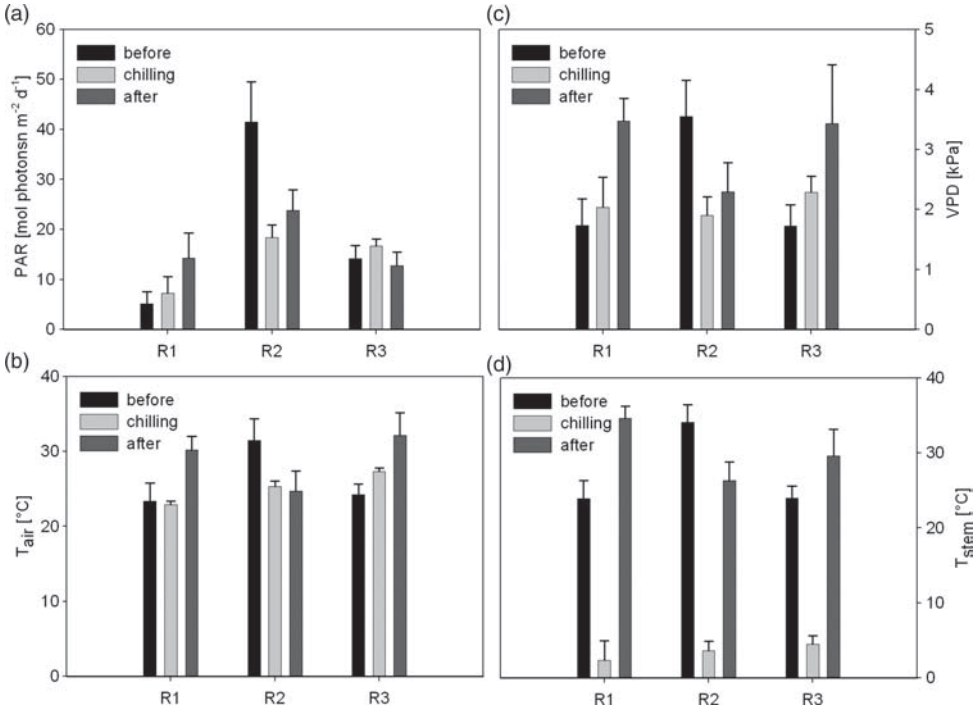

Figure 2. Microclimatic dynamics during the three repetitions (R1, R2 and R3) of the chilling experiment: daily PAR (a), average (from 11:00 till 17:00) air temperature (T_{air}) (b), average (from 11:00 till 17:00) VPD (c) and average (from 11:00 till 17:00) stem temperature (T_{stem}) (d). These data represent the mean (±SE) of all days in the period before, during and after local stem chilling.

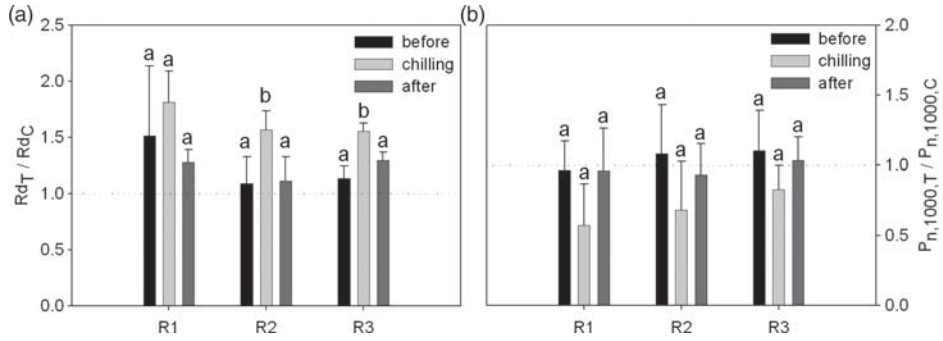

Figure 3. Ratio of average dark respiration ($R_{d,T}$) (a) and net photosynthesis rate at 1000 PAR ($P_{n,1000,T}$) (b) of chilled trees to control trees ($R_{d,C}$ or $P_{n,1000,C}$) during the three repetitions (R1, R2 and R3). Data represent the mean ± SE of five control and five chilled trees measured on 4–5 days per period (before, during and after local stem chilling). Significant differences ($P < 0.20$) per period (before, chilling, after) are indicated by different letters.

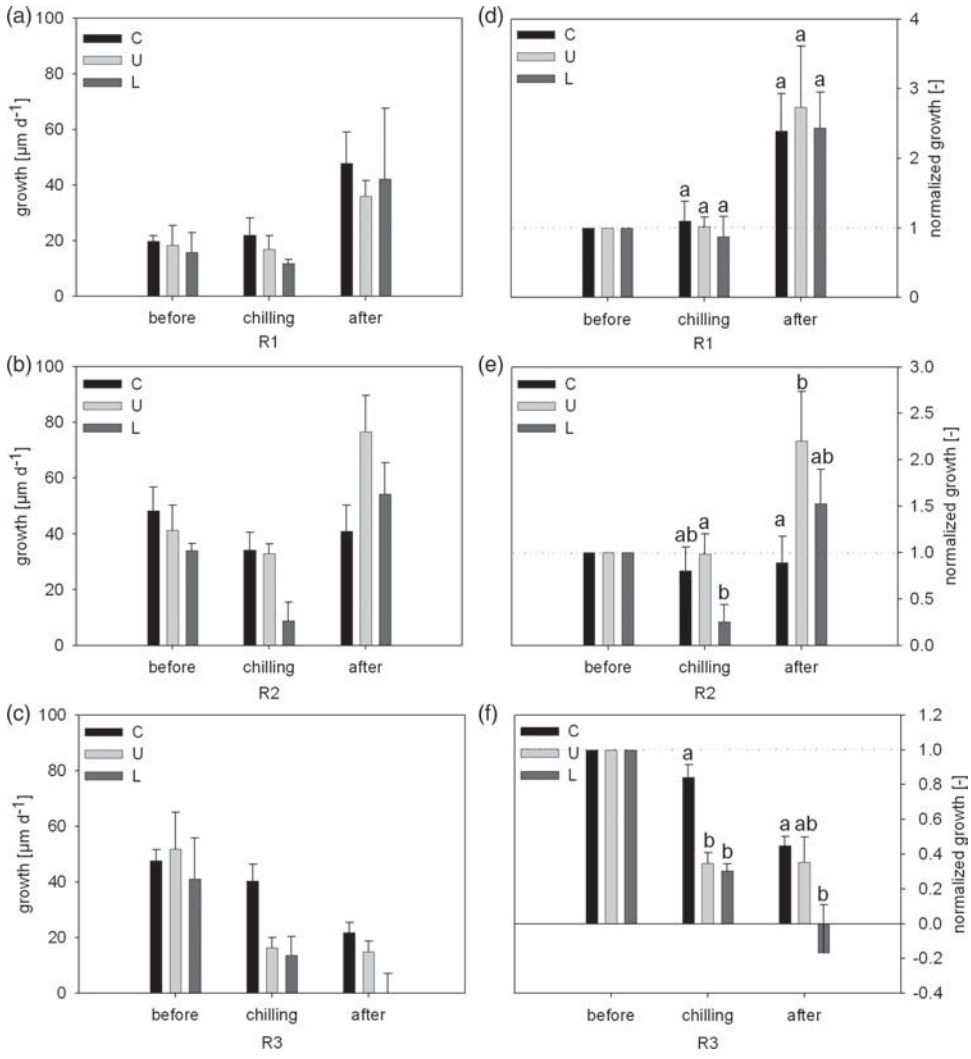

Figure 4. Average growth rate (a–c) and growth rate normalized to the period before chilling (d–f) of the control trees (*C*) and of the stem above (*U*) and below (*L*) the chilled zone during the three repetitions (R1, R2 and R3). Data represent the mean ± SE of five control and five chilled trees in the period before, during and after local stem chilling. Significant differences (Tukey, $P \leq 0.05$) per period (before, chilling, after) are indicated by different letters.

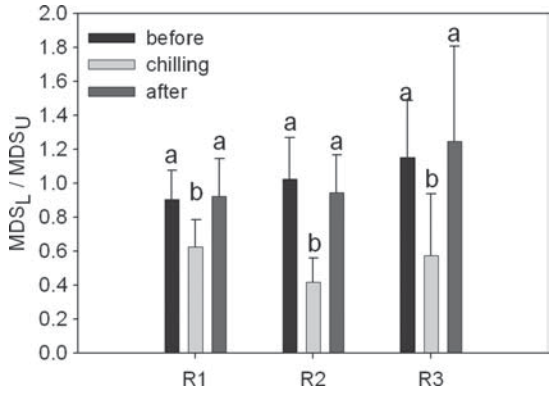

Figure 5. Changes in the ratio between MDS in the stem zone below (*L*) and above (*U*) the chilled zone during the period before, during and after chilling for all three repetitions (R1, R2 and R3). Data represent the mean ± SE of five control and five chilled trees in the period before, during and after local stem chilling. Significant differences (Tukey, $P \leq 0.05$) per period (before, chilling, after) are indicated by different letters.

was significantly higher compared with *L* for all three repetitions.

Carbohydrates

Figure 6 depicts the relative carbohydrate concentrations in the bark during the chilling experiment. It appeared that during R1 the carbohydrates (either sugars or starch) tended to increase over time for both the control and chilled trees, although the effect was not significant. During R2, a significant difference was observed between the relative soluble sugar concentrations in *U* and *L* (Figure 6b). During chilling the sugar concentration increased in *U* and decreased in *L*, making the sugar concentration in *U* significantly higher than in *L*. This discrepancy remained at least 1 week after chilling. A similar trend could be observed in the starch concentration. Due to the large variability in samples, this increase was, however, not significant (Figure 6e). During R3 no significant changes could

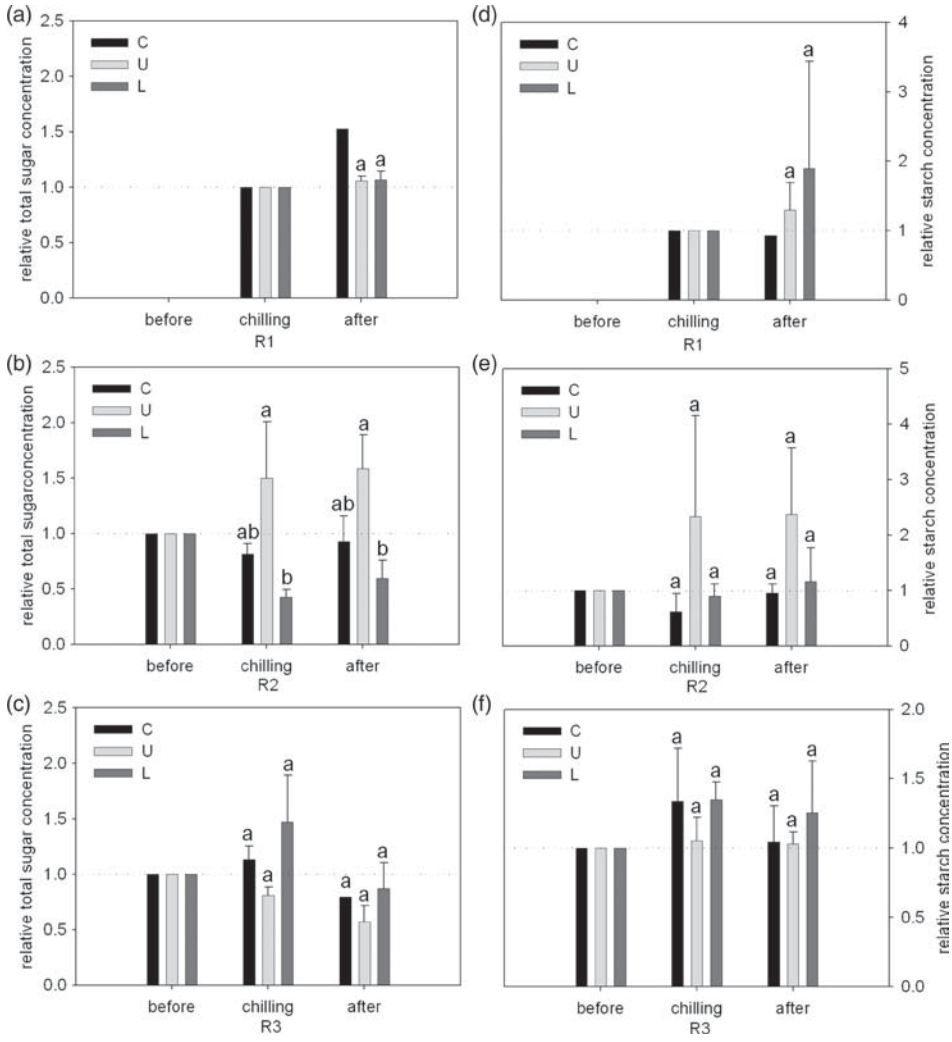

Figure 6. Relative concentration of total soluble sugars (sum of sucrose, sorbitol, glucose and fructose) (a–c) and starch (d–f) in the bark of control trees (*C*) and in the bark above (*U*) and below (*L*) the chilled zone in the period before, during and after chilling for the three repetitions (R1, R2 and R3). Data represent the mean ± SE of two control and two chilled trees in the period before, during and after local stem chilling. Significant differences (Tukey, $P \leq 0.05$) per period (before, chilling, after) are indicated by different letters.

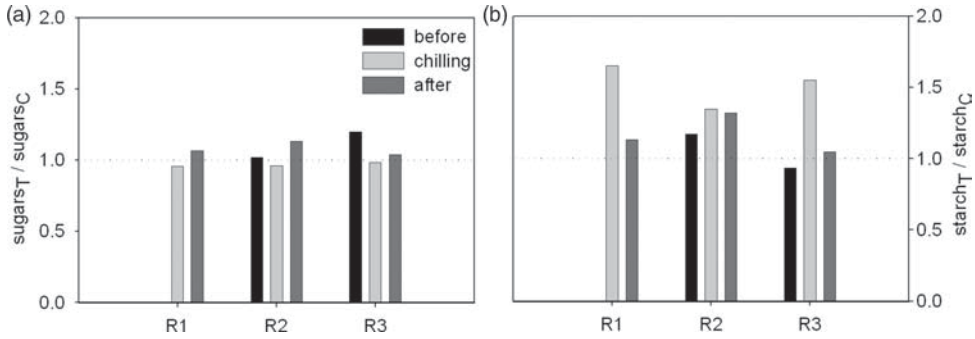

Figure 7. Ratio of total sugar concentration (sum of sucrose, sorbitol, glucose and fructose) (a) and starch (b) of chilled trees (*T*) to control trees (*C*) in the period before, during and after chilling for the three repetitions (R1, R2 and R3).

be detected in the relative carbohydrate concentration (Figure 6c and f). A slight increasing trend in starch could be detected (Figure 6f), while the total sugar concentration tended to decrease for the period after chilling (Figure 6c). For R1 and R2, similarities could be found between the dynamics in relative carbohydrate concentrations (Figure 6d and e) and relative growth rate (Figure 4d and e). Especially in R2, an increase or decrease in relative growth rate was accompanied by an increase or decrease in carbohydrate concentration, respectively. This relationship, however, did not hold for R3.

In the leaves, the ratio of starch concentration between chilled and control trees increased during the chilled period (Figure 7b). An opposite, but smaller, trend was observed for the total sugar concentrations (Figure 7a).

Discussion

Chilling-induced inhibition of photosynthesis in the source leaves

Local stem chilling induced several responses in the source leaves (Figures 3 and 7). Several studies (Iglesias et al. 2002, Cheng et al. 2008, Domec and Pruyn 2008, De Schepper et al. 2010) have indicated that an increased respiration and starch concentration in leaves is related to a feedback inhibition in photosynthesis. In this study, the observed R_d (Figure 3) and starch concentration (Figure 7) increased in the leaves during chilling, while $P_{n,1000}$ (Figure 3) and sugar concentration (Figure 7) tended to decrease. Therefore, the observed changes during chilling indicate that local stem chilling induced a feedback inhibition of photosynthesis in the leaves. These observations are consistent with the measurements of Johnsen et al. (2007), who observed a similar feedback inhibition when trunks of tall pine trees were locally chilled.

The feedback inhibition can be explained by an increased local resistance in the stem phloem due to chilling. Bancal and Soltani (2002) evaluated the temperature dependence of phloem transport resistance, which was originally calculated by Minchin et al. (1993) based on a concentration-driven phloem flow. According to this phloem resistance (Minchin et al. 1993), the temperature alters the resistance not only indirectly by changing the viscosity but also directly. Bancal and Soltani (2002) showed that phloem resistance doubles when temperature drops from 23 to 3 °C (Bancal and Soltani 2002, Peuke et al. 2006). In addition, transport resistance depends on transport length according to the Hagen–Poiseuille equation (Steppe and Lemeur 2007). Therefore, if 5 cm of a 50-cm-long stem is chilled (or 10% of the stem is chilled), the original phloem resistance will increase by 10%:

$$R_{\text{chilling}} = 0.9R_{\text{original}} + 0.1(R_{\text{original}} * 2) = 1.1R_{\text{original}} \quad (1)$$

It is possible that the cold is partially transported upwards with the xylem sap and through vertical conduction. Therefore, the actual chilling length could even be larger than 5 cm, enlarging as such the increased phloem resistance. Observations with magnetic resonance imaging (Peuke et al. 2006) and radioactive ^{11}C labelling (Gould et al. 2004) have shown that local chilling only briefly (several minutes) interrupts phloem flow, and after this interruption phloem flow completely recovers even when chilling still persists. Therefore, the increased phloem resistance (*R*) will probably alter the phloem pressure differences (ΔP) to maintain the phloem flow (*F*) during cooling according to the following equation (De Schepper and Steppe 2010):

$$\Delta P(\uparrow) = F\,R(\uparrow) \quad (2)$$

Such a change in pressure difference was also observed in vivo when local chilling was applied in bean (Gould et al. 2004): the pressure increased above the cold block and decreased below the cold block. It can be hypothesized that this increased pressure above the cold block induced the feedback inhibition in photosynthesis by altering the pressure-dependent phloem loading, as was illustrated in a modelling study using physical girdling (De Schepper and Steppe 2011).

Chilling-induced changes in radial stem growth rate and carbohydrate concentration near the chill

Chilling changed both stem growth rate (Figure 4) and bark carbohydrate concentration (Figure 6). These effects varied across the growing season: they were significant yet very different in R2 and R3, and negligible in R1.

During the chilling period of R2, stem growth above the girdled zone was not hampered by the cold temperature and accompanied by an increase in carbohydrate concentration. In contrast, radial stem growth and carbohydrate concentration decreased below the girdled zone during this period. It seems that local stem chilling resulted in a surplus of available assimilates for growth above the chilled zone and a decrease below. Similar changes in carbohydrate concentrations were also observed by others (Peuke et al. 2006, Johnsen et al. 2007). Two different hypotheses are considered to explain these observations. Firstly, according to the leakage-retrieval mechanism, carbohydrates are continuously leaking out of the phloem tubes and afterwards again retrieved in the tubes. It has been speculated (Lang and Minchin 1986, Peuke et al. 2006) that cold temperatures during stem chilling locally inhibit active retrieval of carbohydrates into the phloem tubes. Due to this inhibited retrieval, sucrose in the apoplast increases in the cold zone, accelerating the lateral carbohydrate transport towards the long-term symplastic buffer. This causes a decrease in sugars available for downward phloem transport. Hence, carbohydrate availability increases in and above the chilled zone and decreases below it. However, this hypothesis is questionable since an absence of starch and sugar accumulation in the cold zone has been reported (Hannah et al. 2001, Peuke et al. 2006). Therefore, another hypothesis has been suggested: the changes in carbohydrate availability were caused by the locally doubled phloem resistance induced by the low chilling temperatures as suggested earlier. The osmotic potential and carbohydrate concentration will increase in the sieve tubes above the chilled zone due to the higher phloem resistance. Accordingly, the lateral leakage of carbohydrates out of the phloem towards the long-term symplastic buffer will increase above the chilled zone, since it is assumed that the leakage process obeys diffusion-like kinetics (Lacointe and Minchin 2008, De Schepper and Steppe 2010). Below the chilled zone the opposite will happen: the osmotic potential and the corresponding lateral leakage will decrease. A similar response was found when phloem resistance was increased by physical girdling (De Schepper and Steppe 2011). This explanation requires increased carbohydrate concentrations in the conductive phloem tubes above the chilled zone during chilling, but this behaviour has until now not been demonstrated (Gould et al. 2004).

At the end of the growing season (R3), the chilling effects in the adjacent stem parts were quite different from the chilling effects observed during the middle of the growing season (R2). Local stem chilling enhanced stem growth cessation both above and below the chilled zone, but the effect was most pronounced below the girdled zone where growth even became negative after chilling. Near the end of the growing season, the drop in temperature apparently halted cambial activity (Tanino et al. 2010). The changes in stem growth did no longer correspond with the carbohydrate concentrations in the bark. Since stem growth dropped the most below the girdled zone, one would expect lower carbon availability below the chilled zone.

The chilling effects on radial stem growth and carbohydrate concentration differed across the growing season and were most significantly observed in the middle of the growing season. In the beginning and at the end of the growing season, the onset and stagnation of stem growth provoked probably too many other changes in such a way that the chilling-induced changes became difficult to unambiguously distinguish and interpret.

Chilling-induced changes in MDS

In the stem adjacent to the chilled zone, effects on MDS were observed (Figure 5). It is possible that due to transpiration the cold is transported upwards, cooling down the stem where the LVDT was positioned. Based on the thermal expansion coefficient of wood (9.395×10^{-5} K^{-1}; Génard et al. 2001) and the dimensions of the studied oak stems (diameter of 1.2 cm), the maximum theoretically calculated diameter shrinkage induced by a temperature drop of 20 °C is 22 µm. In contrast, the observed differences between MDSs of the stem above and below the girdled zone were a factor of 10 larger. Therefore, thermal contraction of the wood could not account quantitatively for the observed differences in MDS. The larger MDS values above the chilled zone suggest that the cold temperatures induced locally a higher xylem hydraulic resistance. Temperature has a known effect on the viscosity and density of pure water (Forsythe 1959). As such, the hydraulic resistance in the Hagen–Poiseuille equation will locally increase by a factor of 1.73 when the stem is cooled from 23 to 3 °C. This local increase of 73% in xylem resistance most likely induced a local perturbation in the xylem pressure profile: the xylem water potential became more negative above the chilled zone during transpiration (analogous to Eq. (2)). Due to this reduced xylem potential, more water will be depleted from the adjacent elastic stem tissues as the xylem and its adjacent tissues tend to be in equilibrium. Therefore, the higher depletion causes the larger MDS observed in the stem above the chilled zone. This effect can be compared to soil drying, which increases the hydraulic resistance at root level and causes as such a larger MDS in the total stem (Intrigliolo and Castel 2006, De Pauw et al. 2008, De Swaef et al. 2009).

Conclusions

Stem chilling induced a feedback inhibition of photosynthesis in the source leaves and induced changes in radial stem

growth, carbohydrate concentration and MDS in the stem near the chilled zone. It is suggested that the feedback inhibition of photosynthesis was caused by a higher total phloem resistance which was induced by the low temperatures and which affected the loading processes in the leaves. The chilling-induced changes in radial stem growth and the carbohydrate concentration in the stem adjacent to the chilled zone were related to a change in carbon translocation. It is hypothesized that the locally increased phloem resistance changed the phloem osmotic pressures and correspondingly the lateral leakage pattern above and below the chilled zone. These effects were most obvious in the middle of the growing season, while they were dominated by other seasonal-induced changes in the beginning and at the end of the growing season, which made their interpretation ambiguous. Changes in MDS were linked to a higher stem xylem hydraulic resistance induced by the cold temperatures. It can be concluded that localized stem chilling affects several important processes in both the sources and sinks of trees.

Acknowledgments

We are indebted to Philip Deman and Geert Favyts of the Laboratory of Plant Ecology for their accurate and enthusiastic technical support.

Funding

We thank the Research Foundation – Flanders (FWO) for the PhD funding granted to Veerle De Schepper and the postdoctoral fellow funding granted to Lynn Vanhaecke.

References

Ayre, B.G., F. Keller and R. Turgeon. 2003. Symplastic continuity between companion cells and the translocation stream: Long-distance transport is controlled by retention and retrieval mechanisms in the phloem. Plant Physiol. 131:1518–1528.

Bancal, P. and F. Soltani. 2002. Source-sink partitioning. Do we need Munch? J. Exp. Bot. 53:1919–1928.

Cheng, Y.H., O. Arakawa, M. Kasai and S. Sawada. 2008. Analysis of reduced photosynthesis in the apple leaf under sink-limited conditions due to girdling. J. Jpn. Soc. Hortic. Sci 77:115–121.

De Pauw, D.J.W., K. Steppe and B. De Baets. 2008. Identifiability analysis and improvement of a tree water flow and storage model. Math. Biosci. 211:314–332.

De Schepper, V. and K. Steppe. 2010. Development and verification of a water and sugar transport model using measured stem diameter variations. J. Exp. Bot 61:2083–2099.

De Schepper, V. and K. Steppe. 2011. Tree girdling responses simulated by a carbon and water transport model. Ann. Bot. 108:1147–1154.

De Schepper, V., K. Steppe, M.C. Van Labeke and R. Lemeur. 2010. Detailed analysis of double girdling effects on stem diameter variations and sap flow in young oak trees. Environ. Exp. Bot 68:149–156.

De Swaef, T., K. Steppe and R. Lemeur. 2009. Determining reference values for stem water potential and maximum daily trunk shrinkage in young apple trees based on plant responses to water deficit. Agric. Water Manag. 96:541–550.

Domec, J.C. and M.L. Pruyn. 2008. Bole girdling affects metabolic properties and root, trunk and branch hydraulics of young ponderosa pine trees. Tree Physiol. 28:1493–1504.

Forsythe, W.E. 1959. Smithsonian physical tables. Smithsonian Institution, Washington.

Gamalei, Y.V. 2002. Assimilate transport and partitioning in plants: approaches, methods, and facets of research. Russ. J. Plant Physiol. 49:16–31.

Génard, M., S. Fishman, G. Vercambre, J.-G. Huguet, C. Bussi, J. Besset and R. Habib. 2001. A biophysical analysis of stem and root diameter variations in woody plants. Plant Physiol. 126:188–202.

Gould, N., P.E.H. Minchin and M.R. Thorpe. 2004. Direct measurements of sieve element hydrostatic pressure reveal strong regulation after pathway blockage. Funct. Plant Biol. 31:987–993.

Hannah, M.A., M.J. Iqbal and F.E. Sanders. 2001. Adaptation to long-term cold-girdling in genotypes of common bean (*Phaseolus vulgaris* L.). J. Exp. Bot. 52:1123–1127.

Iglesias, D.J., I. Lliso, F.R. Tadeo and M. Talon. 2002. Regulation of photosynthesis through source: sink imbalance in citrus is mediated by carbohydrate content in leaves. Physiol. Plant. 116:563–572.

Intrigliolo, D.S. and J.R. Castel. 2006. Usefulness of diurnal trunk shrinkage as a water stress indicator in plum trees. Tree Physiol. 26:303–311.

Johnsen, K., C. Maier, F. Sanchez, P. Anderson, J. Butnor, R. Waring and S. Linder. 2007. Physiological girdling of pine trees via phloem chilling: proof of concept. Plant Cell Environ. 30:128–134.

Lacointe, A. and P.E.H. Minchin. 2008. Modelling phloem and xylem transport within a complex architecture. Funct. Plant Biol. 35:772–780.

Lalonde, S., M. Tegeder, M. Throne-Holst, W.B. Frommer and J.W. Patrick. 2003. Phloem loading and unloading of sugars and amino acids. Plant Cell Environ. 26:37–56.

Lang, A. and P.E.H. Minchin. 1986. Phylogenetic distribution and mechanism of translocation inhibition by chilling. J. Exp. Bot. 37:389–398.

McQueen, J.C., P.E.H. Minchin, M.R. Thorpe and W.B. Silvester. 2005. Short-term storage of carbohydrate in stem tissue of apple (*Malus domestica*), a woody perennial: evidence for involvement of the apoplast. Funct. Plant Biol. 32:1027–1031.

Minchin, P.E.H. and M.R. Thorpe. 1987. Measurement of unloading and reloading of photo-assimilates within the stem of bean. J. Exp. Bot. 38:211–220.

Minchin, P.E.H., M.R. Thorpe and J.F. Farrar. 1993. A simple mechanistic model of phloem transport which explains sink priority. J. Exp. Bot. 44:947–955.

Münch, E. 1930. Die Stoffbewegunen in der Pflanze. Gustav Fischer, Jena, 234 p.

Peuke, A.D., C. Windt and H. Van As. 2006. Effects of cold-girdling on flows in the transport phloem in *Ricinus communis*: is mass flow inhibited? Plant Cell Environ. 29:15–25.

Pollet, B., L. Vanhaecke, P. Dambre, P. Lootens and K. Steppe. 2011. Low night temperature acclimation of Phalaenopsis. Plant Cell Rep. 30:1125–1134.

Steppe, K. and R. Lemeur. 2004. An experimental system for analysis of the dynamic sap-flow characteristics in young trees: results of a beech tree. Funct. Plant Biol. 31:83–92.

Steppe, K. and R. Lemeur. 2007. Effects of ring-porous and diffuse-porous stem wood anatomy on the hydraulic parameters used in a water flow and storage model. Tree Physiol. 27:43–52.

Tanino, K.K., L. Kalcsits, S. Silim, E. Kendall and G.R. Gray. 2010. Temperature-driven plasticity in growth cessation and dormancy development in deciduous woody plants: a working hypothesis suggesting how molecular and cellular function is affected by temperature during dormancy induction. Plant Mol. Biol. 73:49–65.

Thorpe, M.R., A.C.U. Furch, P.E.H. Minchin, J. Foller, A.J.E. Van Bel and J.B. Hafke. 2010. Rapid cooling triggers forisome dispersion just before phloem transport stops. Plant Cell Environ. 33:259–271.

Thorpe, M.R., P.E.H. Minchin, N. Gould and J.C. McQueen. 2005. The stem apoplast: a potential communication channel in plant growth regulation. *In* Vascular Transport in Plants. Eds. N.M. Holbrook and M.A. Zwieniecki. Elsevier, Burlington, pp 355–371.

van Bel, A.J.E. 2003*a*. Phloem transport: the collective power of single modules. *In* Physiological Plant Ecology. Ed. W. Larcher. Springer, Berlin, pp 151–155.

van Bel, A.J.E. 2003*b*. The phloem, a miracle of ingenuity. Plant Cell Environ. 26:125–149.

van Bel, A.J.E. 2003*c*. Transport phloem: low profile, high impact. Plant Physiol. 131:1509–1510.